

Near-Room-Temperature Production of Diameter-Tunable ZnO Nanorod Arrays through Natural Oxidation of Zinc Metal

Zhongping Zhang,^[a] Haidong Yu,^[b] Xiaoqiong Shao,^[b] and Mingyong Han*^[a, b]

Abstract: A simple, low-temperature strategy has been developed for the low-cost and large-area fabrication of ZnO nanoarrays on a zinc substrate by the natural oxidation of zinc metal in formamide/water mixtures. The one-step, wet-chemical approach has exhibited well-controlled growth of highly oriented and densely packed ZnO

nanoarrays with large-area homogeneity and consisting of nanorods or nanowires with predictable morphologies, such as tunable diameters and identical

Keywords: nanorods • nanostructures • nanowires • oxidation • zinc oxide

lengths. The chemical-liquid-deposition process, an analogue to the widely used chemical-vapor-deposition technique, has been used for the near-room-temperature production of ZnO nanoarrays through continuous supply, transport, and thermal decomposition of zinc complexes in a liquid phase.

Introduction

Nanostructured zinc oxide (ZnO) with diverse morphologies, such as nanowires, nanorods, nanobelts, nanotubes, and nanorings, has been extensively studied due to its unique physical properties, including its wide band gap and large excitonic binding energy at room temperature; such properties suggest promising applications in short-wavelength optoelectronic devices, solar energy conversion, transparent conducting coating materials, and sensors.^[1–11] The recent demonstration of room-temperature ultraviolet lasing from well-oriented ZnO nanowire or nanorod arrays (nanoarrays) has further stimulated substantial efforts to develop methodologies for the synthesis of one-dimensional ZnO nanostructures to be used for constructing electronic and optoelectronic devices.^[1] Among the various techniques reported in the literature, two vapor-phase-deposition techniques are the most popular for high-temperature growth of high-quality ZnO nanoarrays, but are also energy-consuming. Simple physical vapor deposition generally requires an economical-

ly prohibitive high temperature ($> 800\text{ }^{\circ}\text{C}$),^[12–15] and complex chemical vapor deposition involves expensive substrates, sophisticated equipment, and rigorous experimental conditions, although the organometallic zinc precursors used can reduce the reaction temperature to $400\text{ }^{\circ}\text{C}$.^[16–19] Recently, low-temperature ($90\text{--}95\text{ }^{\circ}\text{C}$) preparation of homogeneous and dense ZnO nanoarrays has also been achieved through a two-step, wet-chemical process, which includes the coating of a substrate with ZnO seed particles and the thermal decomposition of Zn-amide complexes in a mixed zinc salt/amide aqueous solution.^[4,20–22] However, it is still a challenge to develop a simple, mild, and practical strategy for the low-cost and large-area fabrication of high-quality ZnO nanoarrays; such a strategy is in great demand for use in promising applications.

Here, we report the near-room-temperature production of highly oriented and densely packed ZnO nanoarrays by using the very simple, natural oxidation of zinc metal in a mixture of formamide and water; the process is based on heterogeneous nucleation and subsequent crystal growth of 1D nanostructures on the zinc substrate. This direct, one-step approach allows the well-controlled growth of high-quality, well-aligned ZnO nanoarrays with large-area homogeneity and consisting of nanowires or nanorods with predictable morphologies, such as identical lengths and tunable diameters. Such diameter-tunable 1D ZnO nanostructures, ranging from tens to hundreds of nanometers, can be achieved by systematically adjusting the volume content of formamide in water, by which the controlled supply rate of zinc reactants can be continuously adjusted.

[a] Dr. Z. P. Zhang, Prof. Dr. M. Y. Han
Institute of Materials Research and Engineering
3 Research Link, Singapore 117602 (Singapore)
Fax: (+65) 6872-0785
E-mail: my-han@imre.a-star.edu.sg

[b] H. D. Yu, X. Q. Shao, Prof. Dr. M. Y. Han
Department of Materials Science
National University of Singapore, Singapore 119260 (Singapore)

This newly developed chemical-liquid-deposition process for the fabrication of ZnO nanoarrays through the continuous supply, transport, and thermal decomposition of organometallic zinc precursors in the liquid-phase is similar to the widely used chemical-vapor-deposition technique. The simple, self-seeding growth of ZnO nanoarrays not only has an attractive low temperature, but also avoids the use of exotic metals or metal oxides as catalysts or seed particles, respectively. Like chemical vapor deposition, highly pure zinc metal is used as the zinc source, which can also avoid introducing impurities, such as counterions, from Zn salts that are often involved in other wet-chemical approaches. The exclusion of exotic metal catalysts and counterions is very important for fabricating reliable devices, because even very low concentrations of impurity could cause dopant species to be incorporated in semiconductor nanorods, and thus generate unintentional defect levels and significantly affect the device properties. In addition to the production of large areas of ZnO nanoarrays with diameter-tunable nanorods, this simple strategy can also be developed for the fabrication of nanostructures of other transition-metal oxides.

Results and Discussion

When the zinc substrate is simply immersed into a formamide/water mixture for 24 h at temperatures as low as 45 °C, the spontaneous chemical liquid deposition and growth of ZnO nanorods on it is sparse, because foreign seed particles were not introduced onto the substrate. However, at an optimized temperature of 65 °C high-quality ZnO nanoarrays can be produced readily by this simple approach. Figure 1 shows the well-aligned nanorod array with large-area homogeneity that was grown on a zinc substrate in 5% formamide/water at 65 °C for 24 h. The uniform nanorods, with an average diameter of ~140 nm, were densely packed on the substrate. The flat-surface appearance of the nanorod array indicates the uniform length of the nanorods. The well-facet-

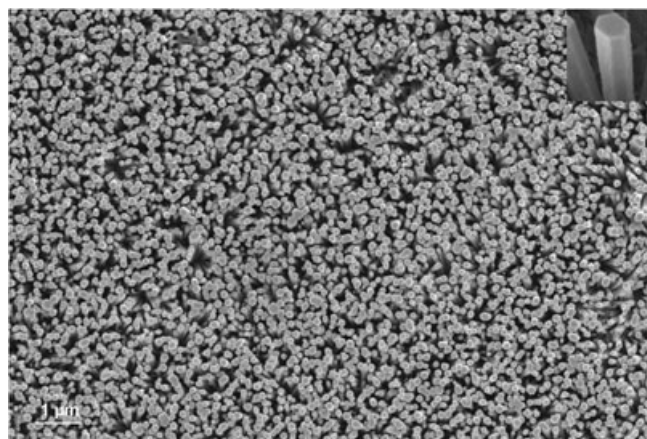


Figure 1. Scanning electron microscopy (SEM) image of a ZnO nanorod array grown on a zinc substrate immersed in formamide/water (5% v/v) at 65 °C for 24 h.

ed end and side surfaces of the hexagonal nanorods is also shown clearly in Figure 1 (inset image).

The presence of wurtzite ZnO was identified by analysis of the X-ray diffraction (XRD) pattern of the nanorod array (Figure 2A). In addition to the diffraction peaks from the zinc metal, there is only one very strong (002) diffraction peak from the ZnO nanorods, whereas other ZnO peaks are either very weak or not detected. The predominant (002) reflection, with a narrow full width at half maximum of ~0.7°,

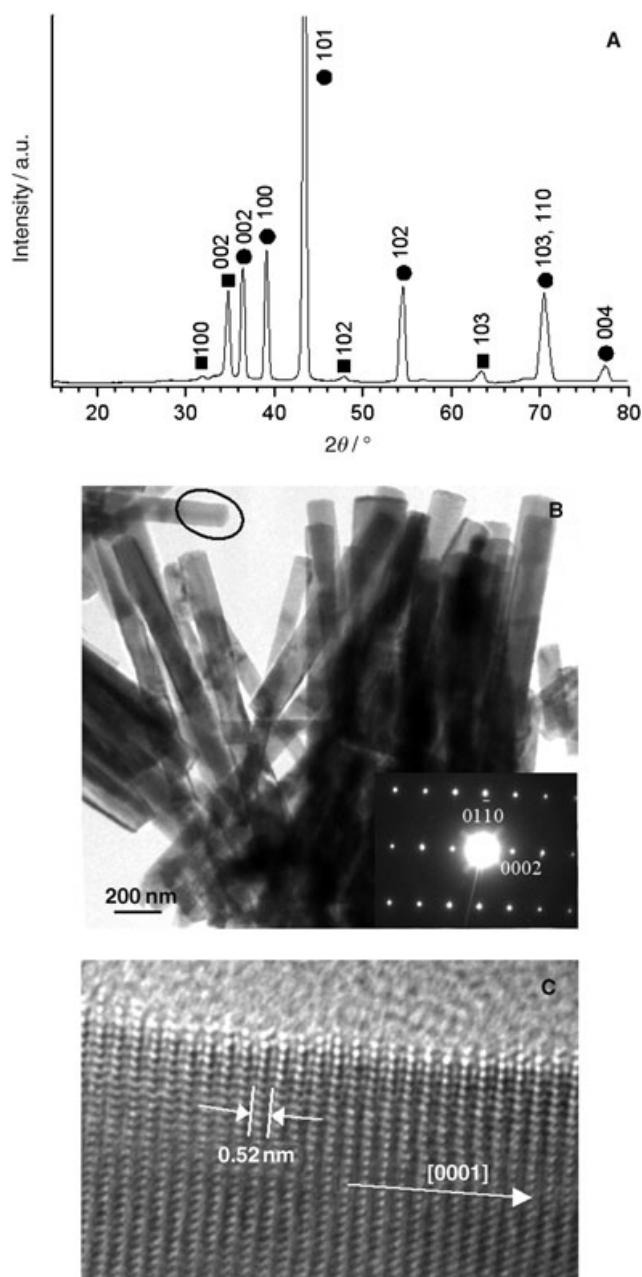
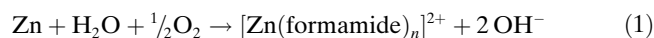


Figure 2. Structural investigation of ZnO nanorods grown on a zinc substrate immersed in a 5% formamide/water mixture. A) X-ray diffraction pattern of a highly oriented array of ZnO nanorods (■: hexagonal ZnO, ●: Zn substrate), B) TEM image of nanorod morphology and SAED pattern of the selected nanorod, and C) high-resolution TEM image of an isolated nanorod, indicated in (B).

indicates the highly preferential growth of the nanorods perpendicular to the zinc substrate and the highly oriented *c*-axis alignment of the nanorods over a large substrate area. Figure 2B shows the transmission electron microscopy (TEM) image of single nanorods carefully removed from the Zn substrate. Each nanorod, $\sim 1.6 \mu\text{m}$ in length, has a uniform diameter along its entire length. The selected-area electron diffraction (SAED) pattern of a single nanorod (inset of Figure 2B) demonstrates the single-crystal nature of nanorods grown along the [0001] direction. Figure 2C shows the high-resolution TEM image of the single nanorod circled in Figure 2B. The lattice spacing of 0.52 nm corresponds to the *d* spacing of the (0001) crystal planes, further confirming (0001) to be the preferential growth direction. The anisotropic growth of the ZnO crystal along the [0001] direction may be caused by the inherent polar properties along the *c* axis. The velocities of crystal growth in different crystallographic planes were reported to be $V_{(01\bar{1}0)} > V_{(01\bar{1}1)} > V_{(0001)} = V_{(000\bar{1})}$.^[23,24] A strong room-temperature photoluminescence spectrum of the resulting ZnO nanoarrays can exhibit near-band-edge emission by using a He–Cd laser as the excitation source.

It is known that the oxidation of zinc metal by naturally dissolved oxygen is very slow in water due to the passive surface layer of oxide. However, in the presence of formamide the spontaneous natural oxidation process can be drastically accelerated at room temperature, releasing zinc ions into the reaction solution (Figure 3, Δ) through the formation of zinc-formamide complexes (Equation 1).



As shown by the data taken at 65°C in Figure 3, more zinc-formamide complexes can be supplied and accumulated

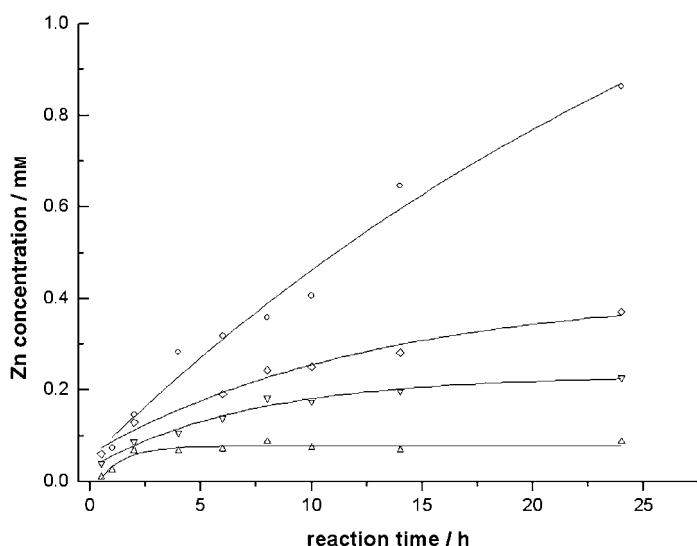


Figure 3. Temporal evolution of zinc concentration in a 5% formamide/water mixture at room temperature (Δ). Temporal evolutions of zinc concentrations in 5 (∇), 10 (\diamond), and 20% (\circ) formamide/water mixtures at 65°C.

continuously by zinc oxidation at an elevated temperature for 24 h. To understand the formation mechanism of ZnO nanorods on the substrate at elevated temperatures, the kinetic process of crystal growth was studied carefully in a 5% formamide/water mixture. In the temporal evolution of zinc oxidation over 24 h at 65°C (Figure 3, ∇) the zinc concentration increased proportionally with reaction time, due to the continuous release of zinc ions into the reaction liquid, and up to 0.23 mmol of Zn complexes were accumulated gradually after 24 h in the formamide/water mixture. As shown too by Figure 3 (∇), the oxidation of the zinc metal in the beginning was very slow, and the resulting low zinc concentration can induce heterogeneous nucleation preferentially on the zinc substrate. By prolonging the reaction time, freshly produced Zn species can be continuously supplied for subsequent crystal growth on the heterogeneous nuclei, by means of thermal decomposition of the resulting Zn-formamide complexes. Figure 4 shows an SEM image of

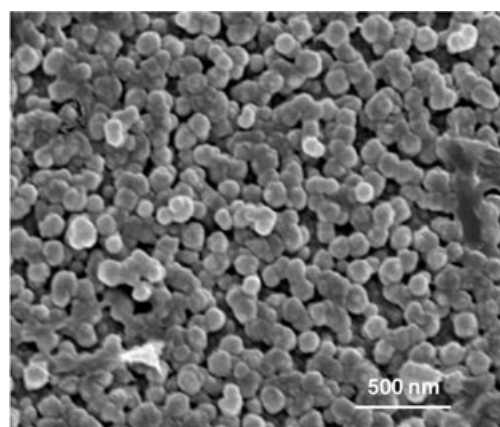


Figure 4. SEM image of ZnO particle seeds grown on a substrate immersed in a 5% formamide/water mixture, after 5 h at 65°C.

a ZnO crystal at an intermediate stage of growth (5% formamide/water after 5 h). An approximate monolayer of uniform ZnO seed particles, $\sim 120 \text{ nm}$ in size, can be seen to have grown on the substrate at this stage. With a further increase in reaction time, these short seed nanoparticles can continuously grow to eventually form ZnO nanorods.

The diameter-tunable growth of ZnO nanorods is demonstrated in Figure 5. Well-oriented ZnO nanorods with different diameters were chemically synthesized on substrates immersed in 2, 5, and 10% formamide/water mixtures. With this increasing formamide content, the average nanorod diameter gradually increased from 50, to 140, to 320 nm, respectively (Figure 5A–C). The average ZnO nanorod diameter is plotted in Figure 6 as a function of formamide content (2, 3, 5, 6, 8, or 10%). The average diameter increased proportionally with the increase in formamide content. This linear relationship demonstrates that the nanorod diameter can be controlled and predicted by simply adjusting the predetermined content of formamide.

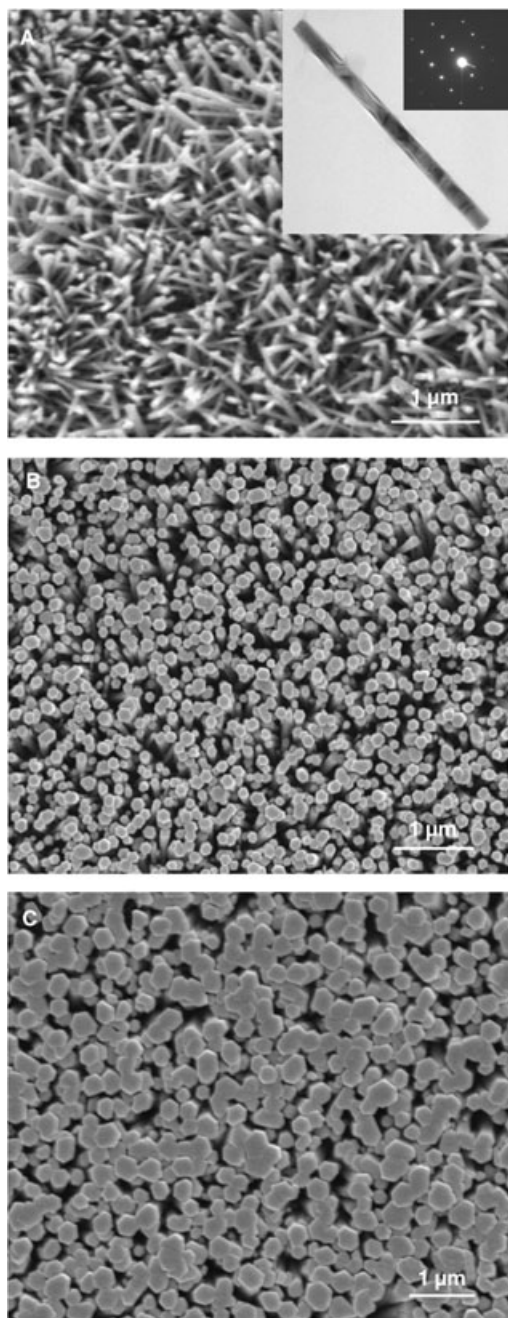


Figure 5. SEM images of ZnO nanorod arrays prepared within 24 h from A) 2, B) 5, and C) 10% formamide/water mixtures. A) Inset shows TEM and SAED images of one single-crystal ZnO nanowire.

The time-dependent evolution of zinc concentration in the reaction solution for different formamide contents was monitored by inductively coupled plasma atomic emission spectrometry (ICP-AES, Figure 3). With an increase of formamide content from 2, 5, 10, 20, to 40%, the zinc concentration increased dramatically after 24 h crystal growth (from 0.12, 0.23, 0.37, 0.86, to 1.49 mM, respectively). This clearly shows that the zinc concentration can be continuously tuned from low to high level by increasing the formamide content in the formamide/water mixture, which enhances

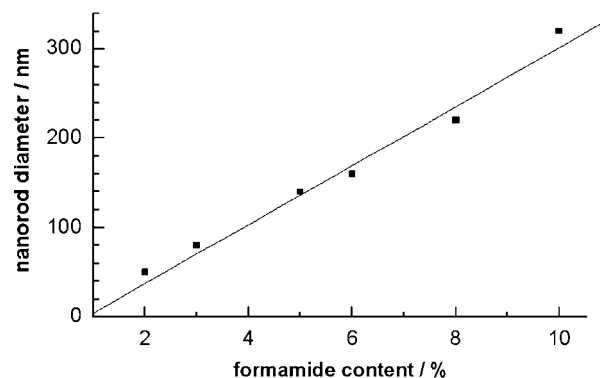


Figure 6. Linear relationship of ZnO nanorod diameter to formamide content.

the oxidation rate of the zinc metal. The increased supply rate of zinc-formamide complexes with increasing formamide content may be the main reason for the formation of thicker nanorods. It was observed that, within the range of 2–10% formamide, ZnO nanorods or nanowires could be grown on the zinc substrate exclusively. When the formamide content was increased twofold, from 10 to 20%, the concentration level of zinc complexes accumulated was much higher, leading to the overgrowth of irregular crystal nanorods on the substrate. It was also noted that the ZnO nanowires produced in a 2% formamide/water mixture had a 50 nm diameter, regular-shaped edges, and a single-crystal wurtzite structure, which grew preferentially along the *c* axis, as shown in the TEM and SAED images of Figure 5A.

When the preparation of ZnO nanorods is carried out at 65 °C, the continuous heterogeneous growth of ZnO nanorods on the Zn substrate can gradually block the dissolution process of the Zn metal. After 24 h, the growth rate is reduced considerably, resulting in the very flat surface of the ZnO nanorod array. On increasing the reaction temperature to 95 °C, the supply rate of zinc precursor can be increased, and a homogeneous nucleation process can occur in solution. The ZnO nanorods obtained at this temperature were not very uniform and the top surface of the nanoarray was also covered with precipitated ZnO aggregates. With increasing reaction time, the Zn substrate was completely converted to ZnO crystals, leading to homogeneous nucleation and growth of nanoparticles in solution.

In the growth mechanism of oriented nanorod arrays, heterogeneous nucleation at the initial stage is crucial for the perpendicular and in-plane alignment of the nanorods. Given that foreign seed particles were not introduced for the growth of ZnO nanorods in the present work, the heterogeneous nucleation may occur at any sites on the substrate for catalyst-free crystal growth. As both Zn and ZnO crystals have hexagonal structures with lattice constants of $a = 0.2665$, $c = 0.4947$ nm and $a = 0.3249$, $c = 0.5206$ nm, respectively, ZnO particles tend to have an epitaxial orientation of lattice planes with the zinc metal base. As shown in Figure 4, the epitaxial heterogeneous nucleation can result in a uniform distribution of ZnO particle seeds on the sub-

strate at the early stage of crystal growth; with their further growth, these seeds can subsequently lead to a uniform distribution of ZnO nanorods on the substrate (Figure 1).

It is generally known that the oriented growth of 1D nanostructures on bare substrates results from the epitaxial relationship between the lattice planes of the nanorods and substrate.^[18] It has also been reported that oriented ZnO nanorods can epitaxially grow on Al₂O₃, with 17% lattice mismatch between nanorod and substrate.^[25] Similarly, it is believed that ZnO particle seeds nucleate and grow epitaxially on a zinc metal substrate, resulting in the perpendicular growth (relative to substrate plane) of nanorods with preferential *c*-axis orientation, because both Zn and ZnO crystals have the same hexagonal structure, with a relatively small lattice mismatch of 4.9 and 18.0% along the *c* and *a* axes, respectively. As shown in Figures 1 and 5, nearly all the nanorods grow perpendicularly from the substrate. For those nanorods that do not grow perpendicularly, their growth may become physically limited as they begin to impinge on neighboring, non-misaligned nanorod crystals, ultimately giving rise to the preferentially oriented nanorod array.

Conclusion

In summary, we report a chemical-liquid-deposition process, as an analogue to the widely used chemical-vapor-deposition technique, for the near-room-temperature growth of ZnO nanoarrays by means of the continuous supply, transport, and thermal decomposition of zinc-formamide complexes. This simple, low-temperature strategy has been developed for the low-cost and large-area fabrication of ZnO nanoarrays, by using the natural oxidation of zinc metal in formamide/water mixtures. This one-step, wet-chemical approach exhibits well-controlled growth of highly oriented and densely packed ZnO nanoarrays, displaying large-area homogeneity and consisting of nanorods or nanowires with predictable morphologies, such as tunable diameters and identical lengths. It is noted that these diameter-tunable ZnO nanowires or nanorods, ranging from tens to hundreds of nanometers, have been achieved by systematically adjusting the volume content of formamide in the formamide/water mixture; this adjustment can continuously alter the supply rate of zinc reactants and control the self-seeding growth of nanoarrays. Room-temperature photoluminescence spectra of ZnO nanoarrays exhibit near-band-edge emission and deep-trap emission. In addition to the large-area production of diameter-tunable ZnO nanoarrays, various nanostructures of transition-metal oxide materials, such as dendritic scaffolds, have been produced by this simple strategy.^[26] In particular, the anisotropic growth of ZnO nanoarrays on arbitrary substrates can be achieved by using evaporated ZnO thin films as buffer layers, which reduce the mismatch between the ZnO nanostructure and substrate.

Experimental Section

Formamide (99.8%, Merck) was used without further purification. Zinc foils (99.9%, Aldrich), 0.127 mm thick, were ultrasonically washed in absolute ethanol before use.

The oxidation of zinc metal and the subsequent growth of ZnO nanorod arrays in formamide/water were carried out in a 4-mL glass vial under atmospheric conditions. In a typical procedure, a piece of zinc foil (7.0 × 7.0 mm) was immersed in water (1.5 mL) containing formamide, the volume content of which ranged from 2 to 10% (v/v). The reaction system was then heated in a drying oven to a constant temperature of 65°C for 24 h. The Zn substrate surface was tarnished gradually due to the formation of a thin layer of white ZnO crystals. The zinc foil was taken out, washed with alcohol and deionized water, and dried at room temperature before characterization.

The size and morphology of the ZnO nanorods were examined by using a JEOL JSM-6700 field-emission scanning electron microscope. X-ray diffraction patterns of nanorod arrays were recorded by using a Bruker AXS GADDS X-ray diffractometer. The nanorod crystalline structure was analyzed by means of a JEOL 3010 transmission electron microscope. The TEM samples were prepared by removing ZnO nanorods from the zinc substrate and dispersing them on a TEM copper grid. The nanorod growth mechanism was studied by monitoring the temporal evolution of Zn concentration in the reaction solution during the 24-h growth period. Zinc concentrations were measured by using inductively coupled plasma atomic emission spectrometry (Optima3000 Perkin–Elmer). Photoluminescence spectra of ZnO nanorod arrays were recorded by using a Bio-Rad 2045 rapid photoluminescence mapping system with a He–Cd laser (325 nm) as the excitation source.

Acknowledgements

This work was supported by the Institute of Materials Research & Engineering and the National University of Singapore.

- [1] M. H. Huang, S. Mao, H. Feick, H. Yan, Y. Wu, H. Kind, E. Weber, R. Russo, P. Yang, *Science* **2001**, *292*, 1897–1899.
- [2] Z. W. Pan, Z. R. Dai, Z. L. Wang, *Science* **2001**, *291*, 1947–1949.
- [3] X. Y. Kong, Y. Ding, R. Yang, Z. L. Wang, *Science* **2004**, *303*, 1348–1351.
- [4] Z. R. Tian, J. A. Voigt, J. Liu, B. Mckenzie, M. J. Mcdermott, M. A. Rodriguez, H. Konishi, H. Xu, *Nat. Mater.* **2003**, *2*, 821–826.
- [5] B. Liu, H. C. Zeng, *J. Am. Chem. Soc.* **2003**, *125*, 4430–4431.
- [6] L. Guo, Y. L. Ji, H. Xu, *J. Am. Chem. Soc.* **2002**, *124*, 14864–14865.
- [7] O. Harnack, C. Pacholski, H. Weller, A. Yasuda, J. M. Wessels, *Nano Lett.* **2003**, *3*, 1097–1101.
- [8] K. Keis, L. Vayssieres, S.-E. Lindquist, A. Hagfeldt, *Nanostruct. Mater.* **1999**, *12*, 487–490.
- [9] T. Minami, *MRS Bull.* **2000**, *25*, 38–44.
- [10] J. T. Hu, T. W. Odom, C. M. Lieber, *Acc. Chem. Res.* **1999**, *32*, 435–445.
- [11] S. C. Minne, S. R. Manalis, C. F. Quate, *Appl. Phys. Lett.* **1995**, *67*, 3918–3920.
- [12] Y. C. Kong, D. P. Yu, B. Zhang, W. Feng, S. Q. Feng, *Appl. Phys. Lett.* **2001**, *78*, 407–409.
- [13] S. J. Chen, Y. C. Liu, J. G. Ma, D. X. Zhao, Z. Z. Zhi, Y. M. Lu, J. Y. Zhang, D. Z. Shen, X. W. Fan, *J. Cryst. Growth* **2002**, *240*, 467–472.
- [14] M. H. Huang, Y. Wu, H. Feick, N. Tran, E. Weber, P. Yang, *Adv. Mater.* **2001**, *13*, 113–116.
- [15] P. X. Gao, Y. Ding, Z. L. Wang, *Nano Lett.* **2003**, *3*, 1315–1320.
- [16] S. C. Lyu, Y. Zhang, C. J. Lee, *Chem. Mater.* **2003**, *15*, 3294–3299.
- [17] J. Wu, S. Liu, *Adv. Mater.* **2002**, *14*, 215–218.
- [18] J. Wu, S. Liu, *J. Phys. Chem. B.* **2002**, *106*, 9546–9551.
- [19] W. I. Park, G. Yi, M. Kim, S. L. Pennycook, *Adv. Mater.* **2002**, *14*, 1841–1843.

- [20] L. E. Greene, M. Law, J. Goldberger, F. Kim, J. C. Johnson, Y. Zhang, R. J. Saykally, P. Yang, *Angew. Chem.* **2003**, *115*, 3139–3142; *Angew. Chem. Int. Ed.* **2003**, *42*, 3031–3034.
- [21] L. Vayssieres, *Adv. Mater.* **2003**, *15*, 464–466.
- [22] Z. R. Tian, J. A. Voigt, J. Liu, B. Mckenzie, M. J. Mcdermott, *J. Am. Chem. Soc.* **2002**, *124*, 12954–12955.
- [23] L. Vayssieres, K. Keis, A. Hagfeldt, S.-E. Lindquist, *Chem. Mater.* **2001**, *13*, 4395–4398.
- [24] W. J. Li, E. W. Shi, W. Z. Zhong, Z. W. Yin, *J. Cryst. Growth* **1999**, *203*, 186–196.
- [25] W. I. Park, D. H. Kim, S. W. Jung, G. C. Yi, *Appl. Phys. Lett.* **2002**, *80*, 4232–4234.
- [26] Z. P. Zhang, X. Q. Shao, H. D. Yu, Y. B. Wang, M. Y. Han, *Chem. Mater.* **2005**, *17*, 332–336.

Received: November 16, 2004
Published online: March 17, 2005